

Electron Microscopic Examination of Wastewater Biofilm Formation and Structural Components

T. TAYLOR EIGHMY,¹* DENISE MARATEA,² AND PAUL L. BISHOP¹

Departments of Civil Engineering¹ and Microbiology,² University of New Hampshire, Durham, New Hampshire 03824

Received 21 January 1983/Accepted 23 March 1983

This research documents in situ wastewater biofilm formation, structure, and physicochemical properties as revealed by scanning and transmission electron microscopy. Cationized ferritin was used to label anionic sites of the biofilm glycocalyx for viewing in thin section. Wastewater biofilm formation paralleled the processes involved in marine biofilm formation. Scanning electron microscopy revealed a dramatic increase in cell colonization and growth over a 144-h period. Constituents included a variety of actively dividing morphological types. Many of the colonizing bacteria were flagellated. Filaments were seen after primary colonization of the surface. Transmission electron microscopy revealed a dominant gram-negative cell wall structure in the biofilm constituents. At least three types of glycocalyxes were observed. The predominant glycocalyx possessed interstices and was densely labeled with cationized ferritin. Two of the glycocalyxes appeared to mediate biofilm adhesion to the substratum. The results suggest that the predominant glycocalyx of this thin wastewater biofilm serves, in part, to: (i) enclose the bacteria in a matrix and anchor the biofilm to the substratum and (ii) provide an extensive surface area with polyanionic properties.

A biofilm may be described as an assemblage of bacterial cells that is both enclosed by and attached to a wetted surface by means of an extracellular fibrous polysaccharide-containing matrix. This matrix, termed a glycocalyx (14), is synthesized by the bacteria, and it serves, in part, to permanently anchor bacterial cells adsorbed to a substratum (24). Wastewater biofilms may be more complex, however, than a simple assemblage of firmly attached bacterial cells; they may possess a thick, overlying, less firmly bound, filamentous bacterial component (1).

Despite the importance of biofilms to a variety of wastewater treatment systems (e.g., rotating biological contactors, fluidized beds), little is known about the initial events of in situ wastewater biofilm formation and its concomitant extracellular structural development. The literature pertaining to wastewater biofilm formation is limited to studies on biofilm-forming activated sludge bacteria grown in laboratory reactors (5, 33, 40, 49). The examinations of the accompanying wastewater biofilm glycocalyx development have been based on inference from ultrastructural examinations of wastewater (6, 26) and adhering polluted stream isolates (29) grown in the laboratory, and adhering marine assemblages (10, 24).

Consequently, this research was conducted to

document the initial events of in situ wastewater biofilm development, using scanning electron microscopy (SEM). Because of the suspected importance of the bacterial glycocalyx in the early events of biofilm formation and the role it may play in regulating substrate transport to metabolically active cells (20), an examination of biofilm structure and its physicochemical properties was made with transmission electron microscopy (TEM). Cationized ferritin (CF) was used to visualize the anionic nature of the biofilm glycocalyx. We describe here a wastewater biofilm formation process that parallels marine biofilm formation. The thin wastewater biofilm was anchored to the substratum by a glycocalyx that possessed interstices, was spatially extensive, and whose anionic sites were densely labeled by CF.

MATERIALS AND METHODS

Preparation of inert substratum. We designed an inert substratum and supporting structure suitable for (i) submersion in a wastestream, (ii) bacterial adhesion, and (iii) subsequent examination by both SEM and TEM. The sampling device is shown in Fig. 1. It consisted of an inert substratum (sampling stub) attached to a nylon screw that was threaded into the wall of a rigid polyvinyl chloride pipe (1.27-cm inner diameter, 50 cm long). The circular sampling stubs (0.316 cm²) were manufactured from flexible polyvinyl chloride tubing (1.27-cm inner diameter) with a 0.635-cm

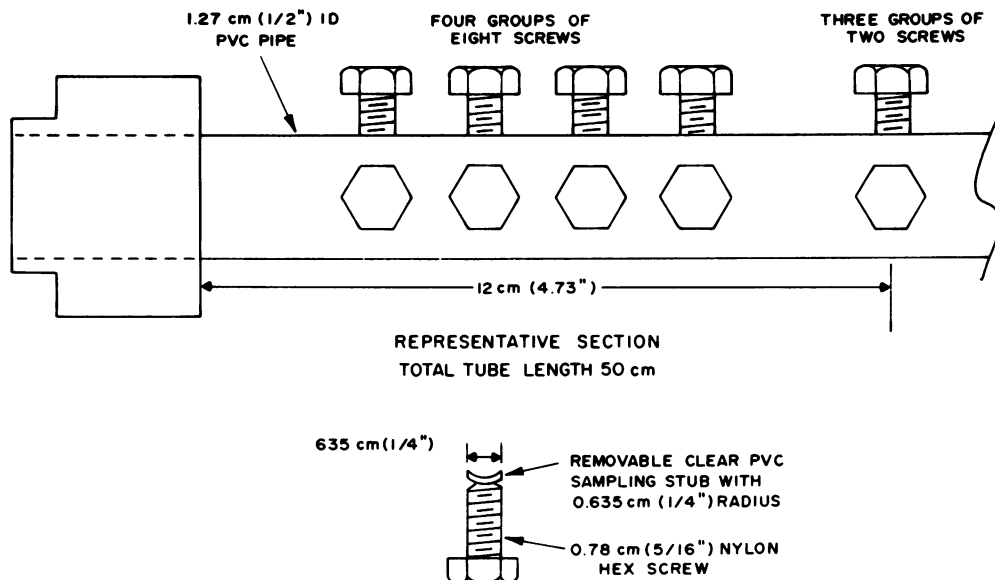


FIG. 1. Schematic of sampling device. Device consists of a support structure (polyvinyl chloride pipe with 38 threaded holes, above) and 38 sampling stubs with screws (one shown, below). Screws with clean attached stubs are threaded into holes in pipe wall so that the pipe interior is hydraulically smooth.

paper hole punch. The sampling stubs, possessing the same curvature as the pipe, were glued to the nylon screws as shown in Fig. 1. The screws were then threaded into the pipe, as shown, and aligned so that the inner pipe surface was hydraulically smooth. Each pipe held 38 screws with sampling stubs. The sampling stub was a hydrophobic plastic (flexible polyvinyl chloride with little or no surface charge) considered suitable for both microbial adhesion (25) and thin-section work.

Biofilm formation was initiated by placing a clean sampling device in a weighted rack and submersing it in a flowing channel at the Durham, New Hampshire, Wastewater Treatment Facility. The channel conveys domestic primary effluent and recycled activated sludge microorganisms to four activated sludge tanks. The rack was oriented in the wastestream so that wastewater could flow through the tubular sampling device. Data on wastewater characteristics were obtained from plant personnel. Dissolved oxygen determinations of the wastewater flow within the channel were made with a YSI model 51A dissolved oxygen meter.

Wastewater biofilm formation studies. Initially, biofilm development was monitored with light microscopy to determine a suitable time frame for electron microscopy work. The optical-focusing, light microscopy method of Characklis et al. (7) was used. Gram stains were conducted on hydrated samples removed from the wastestream at 12-h intervals. Loosely bound filaments were found to coat the stub surface. This layer was easily removed by gentle swirling in distilled water. Underlying, firmly attached bacteria usually covered the stub by 144 h. This time frame was selected as suitable for SEM and TEM studies of the firmly attached component of the biofilm. All samples for SEM and TEM studies were transported to the

laboratory in sealed vials to prevent biofilm desiccation. They were gently swirled in fresh distilled water to remove loosely bound bacteria before fixation (38).

SEM. Samples were prepared for SEM by the methods of McCoy et al. (40). Four stubs were randomly selected from a tubular sampling device at periodic intervals of 24 h. The stubs were rinsed, separated from the nylon screw with a razor, and fixed in 5% glutaraldehyde for 1 h at 20°C. Samples were dehydrated in a graded ethanol series. The stubs and attached biofilm were critical-point dried in a Samdri Critpoint Dryer. The introduction of liquid CO₂ to the drying chamber was manually operated to minimize turbulence. The sampling stubs were glued to specimen holders and sputter coated with a 60:40 gold-palladium mixture. Biofilm specimens were viewed in an AMR 1000 scanning electron microscope at a 20 kV accelerating potential. The specimen stage was tilted to 11° to facilitate photomicrography. Each of the four stub surfaces of each time period was examined and photographed extensively to ensure that a representative sample was obtained.

TEM. Two different fixations were employed to examine the wastewater biofilm glycocalyx in thin section. The first fixation involved prestaining the samples with ruthenium red (RR) by the methods of Cagle et al. (6) before a standard RR fixation (12). The second, separate fixation involved the labeling of anionic functional groups of the biofilm with CF (*N,N*-dimethyl-1,3-propanediamine coupled to horse spleen ferritin; Sigma Chemical Co.) according to a modification of the methods of Danon et al. (15) and MacAlister et al. (36). Controls were fixed without either the RR or the CF. All thin-section work was done on 144-h-old biofilm firmly attached to stub surfaces. Sampling stubs were pretrimmed before fixation to minimize the amount of sampling stub embedded in the resin block

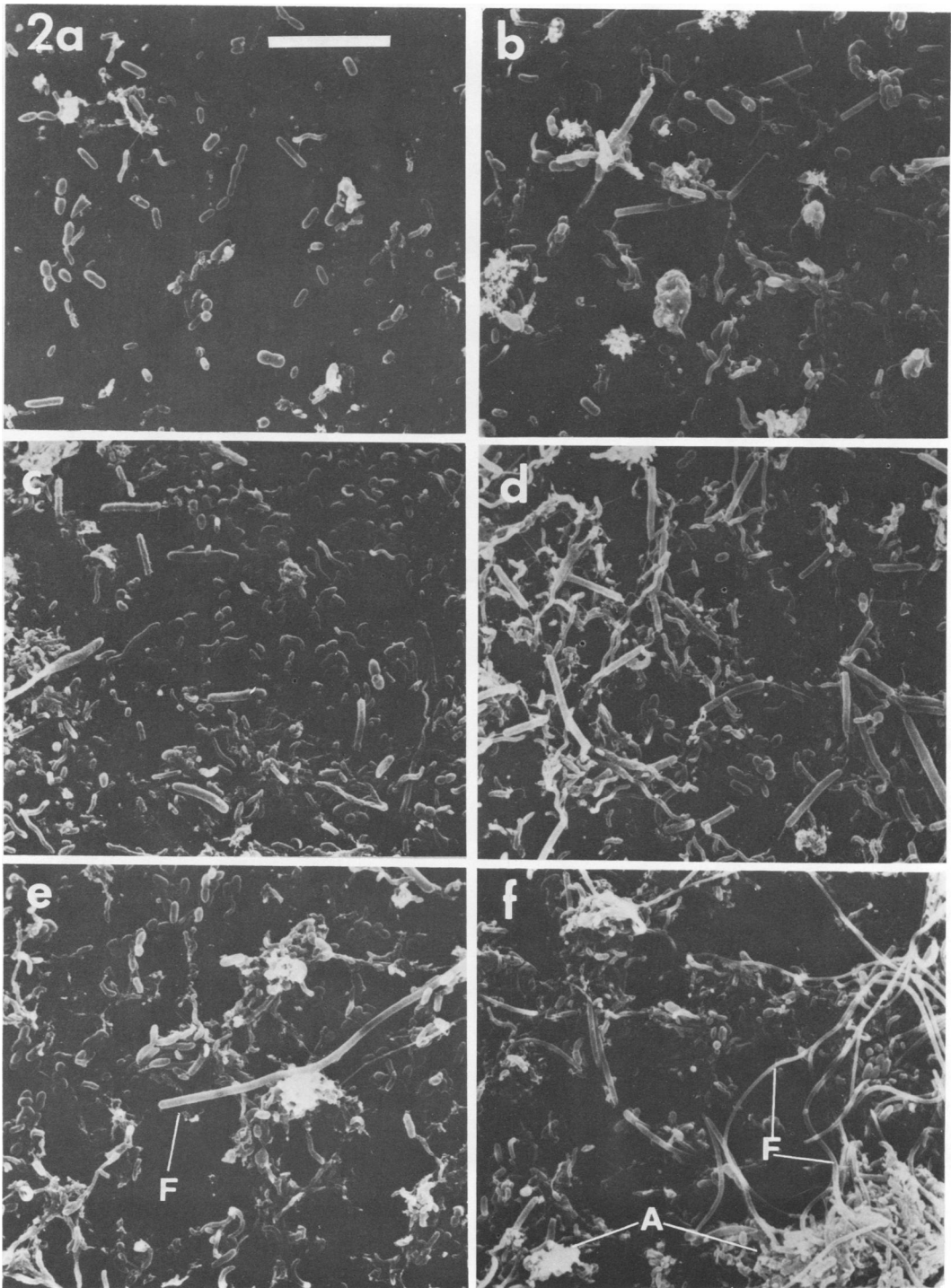


FIG. 2. Representative SEM micrographs showing biofilm development as sampled periodically (every 24 h) up to 144 h. F, filament; A, bacterial aggregate (floc). Bar, 10.0 μm . (a) 24 h, note dividing cells; the black background is the stub surface. (b) 48 h, rod sizes are varied. (c) 72 h. (d) 96 h, cell size is varied. (e) 120 h, note entangled filament. (f) 144 h, extensive clumping and entangled filaments are evident.

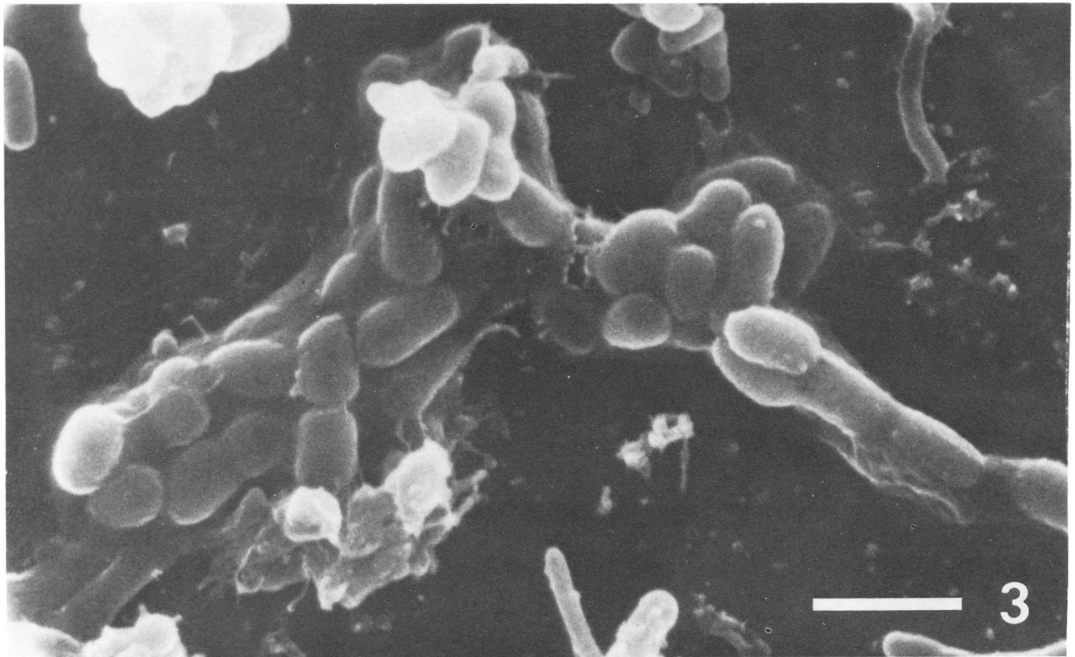


FIG. 3. High-magnification SEM micrograph of microcolony encased in a common capsule. Bar, 2.0 μm . Note morphologically similar cells and the capsule-mediated attachment.

and to facilitate orientation of the biofilm in the block for subsequent examination in thin section.

Samples for the RR fixation were prestained in 0.15% RR for 30 min at 20°C. After washing in 0.1 M cacodylate buffer (CB) with 0.15% RR, the samples were prefixed for 3 h at 20°C in 2.5% glutaraldehyde with CB, 0.15% RR, and 1.0 M sucrose. The samples were subsequently washed in three separate CB solutions with 0.15% RR and decreasing amounts of sucrose (1.0, 0.4, and 0.0 M) for 30 min per wash. Samples were then fixed in 1.0% OsO_4 with CB and 0.15% RR for 3 h at 20°C. Residual OsO_4 was removed with two rinses of CB containing 0.15% RR. A 0.15% RR concentration was maintained through the graded ethanol series to the 50% ethanol concentration to minimize RR leaching (12). The slivers of sampling stubs and attached biofilm were then embedded in a flat mold in Spurr's low-viscosity epoxy resin (47) after a graded infiltration series.

Samples for the CF fixation were washed once with 0.067 M CB (pH 7.2) according to MacAlister et al. (36). Samples were then resuspended in the buffer with the CF at a concentration of 250 $\mu\text{g} \cdot \text{ml}^{-1}$ for 15 min. The samples were gently vortexed at the beginning and end of the 15-min period. Biofilm samples were subsequently washed twice in the CB before additional treatment. The CF samples were prefixed, washed, fixed, washed, dehydrated, and embedded according to the RR procedure with the exception that RR was absent throughout the procedure. Controls were prepared in a manner similar to the RR procedure (prefix through embedding) without the RR.

Thin sections were cut with glass knives on an LKB Ultratome III ultramicrotome. A cutting speed of 2 $\text{mm} \cdot \text{s}^{-1}$ was used. Sections were retrieved on un-

coated, 400-mesh copper grids. Thin sections from the three treatments (RR, CF, and control) were post-stained for 15 min with 0.5% uranyl acetate (in 50% methanol) and for 2 min with 0.4% lead citrate (45). The thin sections were carbon coated for stabilization and viewed with a JEOL JEM-100S transmission electron microscope at an accelerating potential of 80 kV. Numerous thin sections were examined from at least five stubs from each of the fixation procedures. Sections were examined and photographed extensively to ensure that representative samples were obtained. Size measurements of the biofilm were obtained from photographic enlargement of micrographs.

RESULTS

Wastewater characteristics. Influent wastewater flow to the treatment plant during the experimental period averaged 2.31×10^6 liter \cdot day $^{-1}$. The biochemical oxygen demand of the wastewater averaged 183 mg \cdot liter $^{-1}$. The temperature of the wastestream was found to range from 20.0 to 22.5°C. The velocity of flow within the channel where the sampling device was located averaged 0.3 m \cdot s $^{-1}$. Dissolved oxygen values in the wastestream varied between 0.5 and 2.0 mg \cdot liter $^{-1}$ over a diurnal cycle. The inlet end of the sampling tube often became clogged overnight with large suspended solids. Consequently, biofilm development often occurred under static conditions.

Biofilm development—light microscopy. The majority of the attached bacteria in the samples

examined with light microscopy were gram negative. The overlying, loosely bound component contained mostly gram-negative filaments. By 72 h, firmly attached bacteria were usually covered by a common mucoid-like sheet. The mucoid sheet was often extensive. By 144 h, the thickness of the hydrated biofilm was found to average $7 \pm 3 \mu\text{m}$ for three separate stubs (10 observations per stub) as determined by the optical focusing technique (7).

Biofilm development—SEM. We conducted two separate biofilm formation studies with SEM. Both studies showed similar patterns in cell density and diversity. Results from the second study were used. Examinations at lower magnifications revealed uniform biofilm density over a stub surface. Figure 2a through f depicts biofilm development over a 144-h examination period (at 24-h intervals).

A dramatic increase in biofilm cell density was seen over the 144-h period (Fig. 2a through f). The increase in density was a result of both colonization and growth. By 144 h, dense cell clumping was seen, although the stub surface

was not entirely covered. The clumping was also observed in hydrated samples viewed with light microscopy, indicating that the distribution was not an artifact. A variety of bacterial morphologies were observed in all samples. Rod, coccal, spiral, and helical morphologies were seen. Dividing cells were apparent throughout the sampling period (Fig. 2a). Many of the cells possessed flagella. In some instances, bacteria were embedded in an extensive organic layer that may have been similar to the mucoid sheet observed with light microscopy. Many microcolonies were seen embedded in a common capsule. By 144 h of biofilm formation, filaments were a component of the biofilm. These cells were frequently as long as $30 \mu\text{m}$. The filaments were tangled among the underlying, firmly bound component (Fig. 2f). Bacterial flocs, or aggregates, were found attached to the biofilm as well. The bacteria comprising the biofilm appeared to be more clumped (Fig. 2f), rather than being a confluent monolayer of cells.

Figure 3 depicts an attached microcolony of bacterial cells embedded in a common capsule.

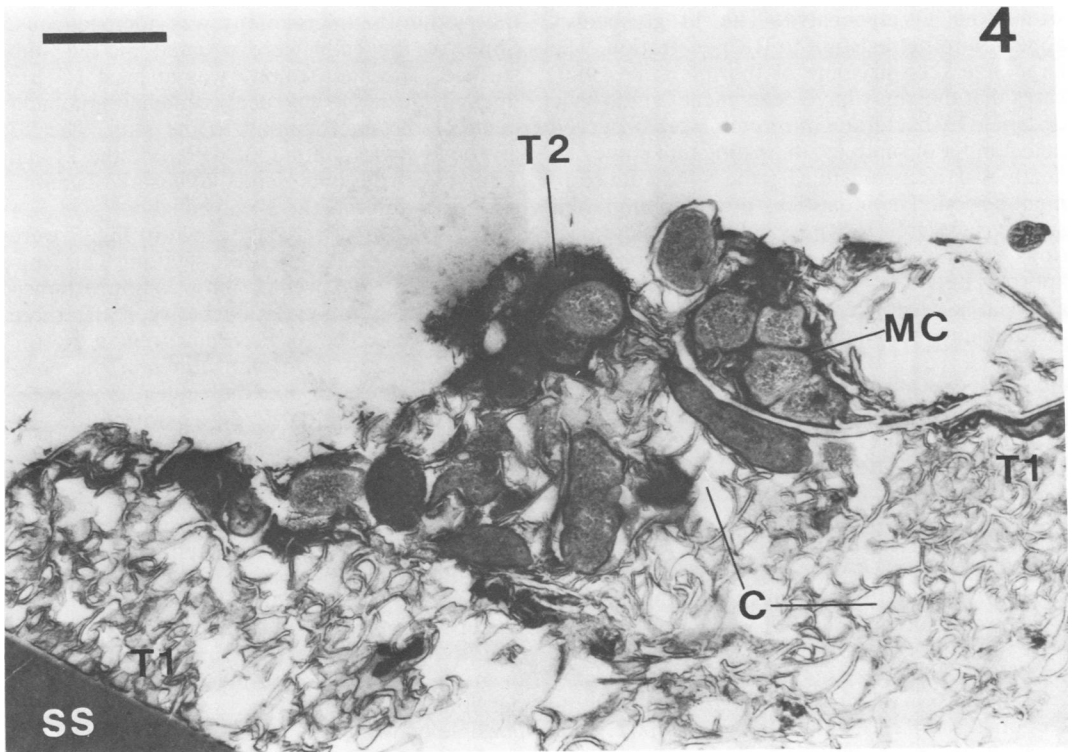


FIG. 4. TEM micrograph of attached biofilm, 144 h old. RR procedure. T1, type 1 glycocalyx; T2, type 2 glycocalyx; MC, microcolony; C, channel within glycocalyx; SS, sampling stub. Bar, $1.0 \mu\text{m}$. Note the glycocalyx-mediated attachment at the stub surface. The spatial arrangement of cells within the glycocalyx matrix is heterogeneous; the interstices provide an extensive surface area.

The capsule encased a large number of bacteria and mediated attachment of the microcolony to the stub surface.

Biofilm structure—TEM. The identification of the structural nature of the fixed and dehydrated wastewater biofilm glycocalyxes reported here was based on the definition of Costerton et al. (14). The capsular portion of the glycocalyx may be "rigid" or "flexible" and either "integral" or "peripheral." The capsular quantity may be further defined by using the prefixes "macro-" or "micro-."

Transmission electron micrographs of thin-sectioned samples (144 h old) fixed with RR (Fig. 4) revealed that the mechanism of biofilm adhesion was mediated by an extracellular matrix that stained positively with RR. The glycocalyx was described (rigid peripheral macrocapsule) and arbitrarily labeled as a type 1 (T1) glycocalyx. The T1 glycocalyx appeared to be spatially extensive and similar to both the mucoid-like blanket seen with SEM and light microscopy and to ones shown elsewhere (18). The T1 glycocalyx possessed interstices. The cross-sectional size of the interstices varied. A clear demarcation was seen between the interstices and their boundary walls (the rigid glycocalyx); suggesting that the interstices may be channels within the T1 glycocalyx. The T1 glycocalyx appeared to be resistant to RR penetration. The large size seen in some of the interstices indicates that they may have been vacant areas once occupied by bacteria. Ghost cells were observed in a number of samples, indicating that some cell death had occurred during the 144-h development period. The interstices provided an extensive surface area for the staining of acidic portions of the glycocalyx (35). It may be more appropriately described as a slime (27). Another glycocalyx was observed (Fig. 4) and described (flexible integral microcapsule) and was delineated as a type 2 (T2) glycocalyx. The T1 and T2 glycocalyxes appeared meshed or continuous as defined by Cheng and Costerton (8). The spatial arrangement of the cells embedded within the T1 glycocalyx was heterogeneous. As shown in Fig. 4, the fixed and dehydrated biofilm appeared to be at least 3.0 μm thick and was similar to the biofilm thicknesses obtained by the optical-focusing technique (7). The cells (Fig. 4) were situated at some distance from the stub surface (>2.0 μm). Some of the cells appeared to comprise a microcolony (8) and may have been dividing.

Transmission electron micrographs of thin-sectioned samples (144 h old) fixed with CF (Fig. 5) revealed results similar to those obtained with the RR technique (Fig. 4). Both T1 and T2 glycocalyxes were observed and appeared to be continuous. The T1 glycocalyx mediated bacte-

rial adhesion to the stub surface and possessed interstices. These provided a large surface area for dense CF deposition. The T1 glycocalyx in Fig. 5 appeared as resistant to CF penetration as the T1 glycocalyx stained with RR (Fig. 4). The low magnification of the micrograph (Fig. 5) was not suitable for examination of specific anionic site labeling. The biofilm in Fig. 5 appeared to be at least 3.0 μm thick.

A high-magnification micrograph (Fig. 6) of a 144-h-old sample prepared by the CF procedure proved suitable for resolving the CF deposition and distribution of anionic sites within a T2 glycocalyx. The CF deposition around the cells was quite dense, again suggesting the flexible (deformable) nature of the microcapsule. In some instances, the CF appeared to penetrate the cytoplasmic membrane of some cells. Some continuity appeared to exist between the T2 glycocalyxes.

A third glycocalyx was described (rigid peripheral macrocapsule) and labeled as a type 3 (T3) glycocalyx. The T3 glycocalyx (Fig. 7) appeared similar to the common capsule seen with SEM (Fig. 3). Some of the cells within the T3 glycocalyx were morphologically similar sister cells (8) and possessed markedly convoluted gram-negative cell envelopes (13). Cell distribution within the microcolony was homogeneous. Some of the cells were situated on the stub surface. The microcolony was at least 1.5 μm thick, with the T3 glycocalyx mediating attachment of the microcolony to the stub. The T3 glycocalyx was continuous with both the T1 and T2 glycocalyxes and seemed to be as resistant to CF penetration as the T1 glycocalyx.

The three glycocalyxes shown in Fig. 7 were obtained from a single thin section. This suggests that sample preparation was not responsible for structural variation between the three glycocalyxes. The intracellular region in the controls did not stain with either of the post-stains or possess CF-like molecules. Large electron-opaque particles were seen within the glycocalyx of one thin-sectioned sample (CF procedure), and they appeared to be quite similar to soil particles (2).

A number of ultrastructural features of the biofilm constituents were seen (not shown). They included: (i) possible poly- β -hydroxybutyrate (PHB) inclusion bodies (21), (ii) possible bacteriophage, (iii) mesosome-like structures (28), (iv) loose membranes similar to those seen in micrographs reported elsewhere (8, 27), (v) possible cyanobacteria ultrastructure, and (vi) possible endospores.

DISCUSSION

This study has documented for the first time the initial events of in situ wastewater biofilm

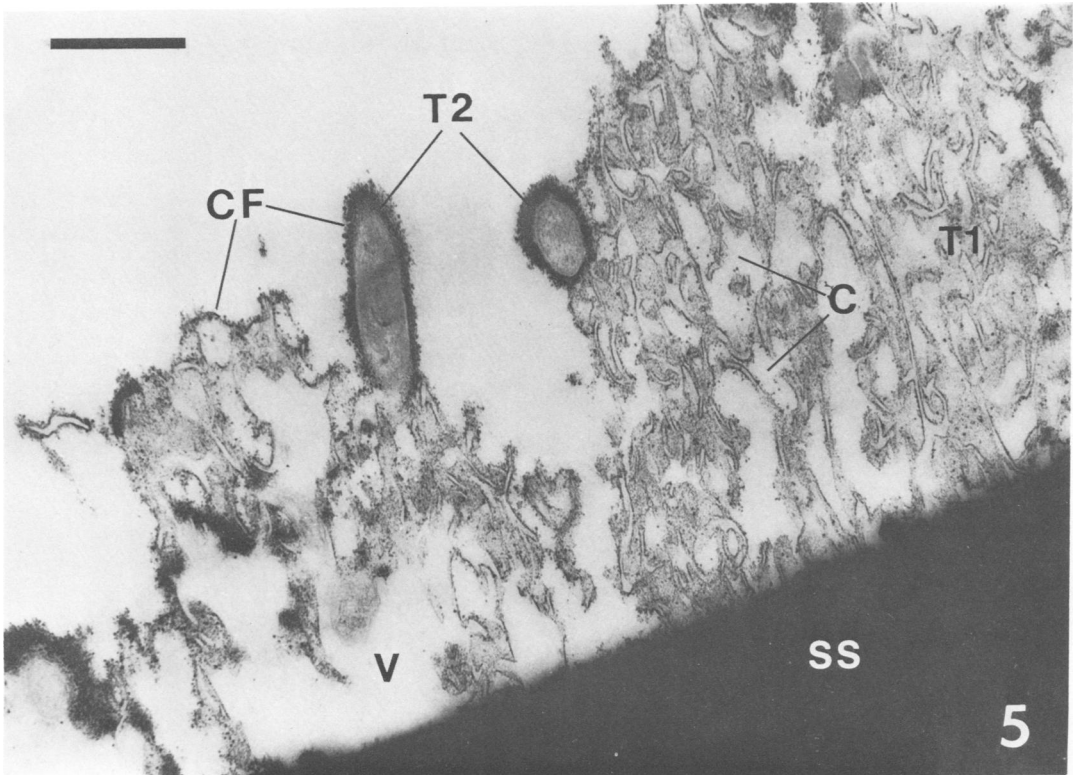


FIG. 5. TEM micrograph of attached biofilm, 144 h old. CF procedure. T1, type 1 glycocalyx; T2, type 2 glycocalyx; CF, CF deposition; C, channels within glycocalyx; V, possible vacant area; SS, sampling stub. Bar, 1.0 μm . Note the glycocalyx-mediated attachment and extensive surface area of channels. The T1 and T2 glycocalyxes are meshed.

formation and concomitant extracellular structural development. This work is significant because prior published work related to these subjects is limited. This study also relates a physicochemical property of the thin wastewater biofilm to its intact extracellular structures.

The nonspecific, permanent adhesion of bacteria to inert surfaces has been thoroughly described for marine bacteria (10, 11, 18, 23, 37). First, the negative surface charge density and wettability of an inert substratum can govern the process of bacterial adsorption. Many environmental conditions will also influence the process (10). A substratum usually adsorbs an organic conditioning film that alters the surficial properties of that substratum (34). Bacterial adsorption requires cell transport to the surface by either motility (37) or fluid eddies (5). Near the substratum, repulsive electrical double-layer forces between the cell and the inert surface are opposed by both attractive London-van der Waals forces and chemical bonding (covalent, hydrophobic, ionic bonds). This phase of adsorption is considered reversible (37). Fimbriae and other adhe-

sive organelles may enhance adsorptivity (10, 42), presumably through polymer bridging. Permanent adhesion usually requires the subsequent synthesis of an acid polysaccharide glycocalyx that connects the adsorbed cell to the conditioned substratum (11, 24). Primary biofilm formation is accomplished primarily by motile, gram-negative rods (11). Secondary biofilm formation involves the incorporation of stalked and filamentous bacteria subsequent to primary biofilm formation (11).

Our research shows that the process of in situ wastewater biofilm development over a 144-h period closely resembles the marine biofilm formation process and the biofilm formation process of wastewater isolates grown in tubular recycle reactors (40). Although a conditioning film was not observed here, a number of primary biofilm colonizers were gram negative and flagellated. The majority of bacteria found in activated sludge systems are thought to be bacteria of this type (19). Such specialized adhesive organelles as fimbriae (10, 42) were not observed, although this does not preclude their

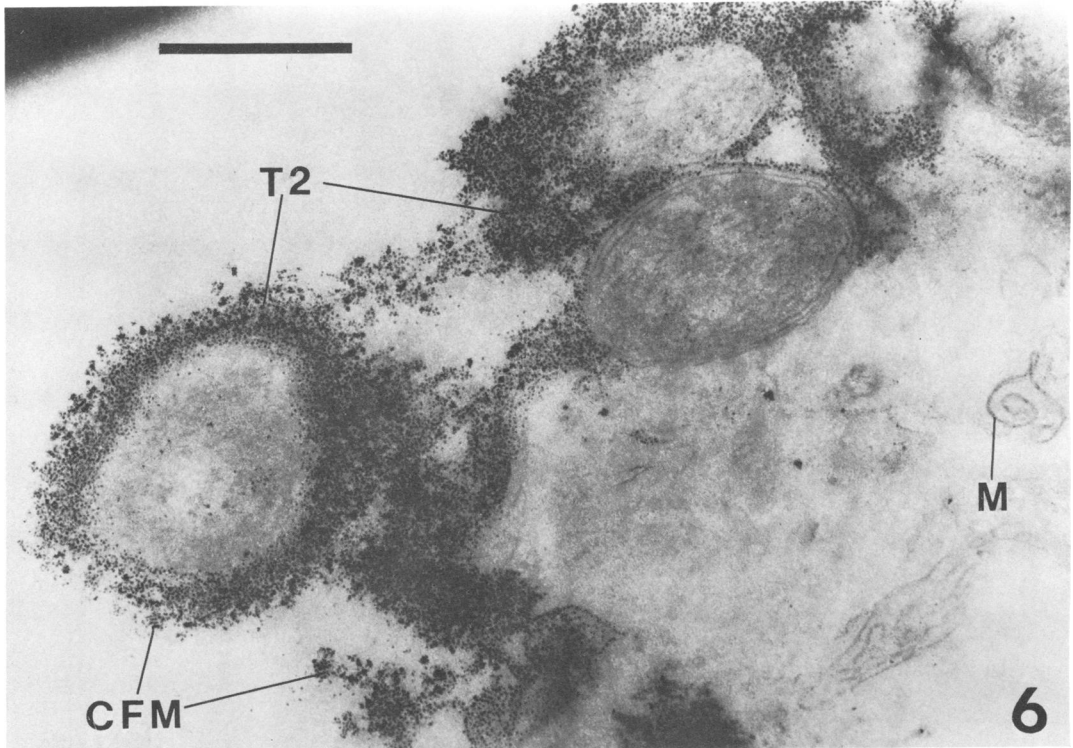


FIG. 6. High-magnification TEM micrograph of 144-h-old biofilm. CF procedure showing extensive anionic charge distribution within apparent type 2 glycocalyx. T2, type 2 glycocalyx; CFM, CF molecules; M, unassociated membranes. Bar, 0.5 μ m. Note the loose membranes in a region of biofilm where the CF did not penetrate.

involvement in wastewater biofilm formation. The presence of an extensive glycocalyx network was seen to form a matrix about the bacteria and anchor the biofilm to the stub surface. This suggests that synthesis of the extracellular material occurred after bacterial adsorption. The inclusion of filamentous bacteria by 144 h of biofilm development indicated secondary biofilm formation. McCoy et al. (40) found that the incorporation of filaments into a wastewater biofilm grown under turbulent conditions first required the presence of a primary biofilm and extensive extracellular polysaccharide. The results presented here indicate that primary biofilm formation provides a textured surface where filaments can entangle and form a thick, overlying layer.

Wastewater biofilms examined in this study were metabolically active with evidence of cell division, microcolonies, cell size variation, and extensive glycocalyx synthesis. A number of hypotheses have been advanced to explain enhanced microbial activity at solid interfaces (22, 32, 52). The extensive glycocalyx synthesis seen here is the most obvious indicator of enhanced

metabolism. Copious glycocalyx synthesis has been correlated with nonlimiting organic carbon concentrations in the growth medium (39, 50, 51) and a decrease in cellular levels of PHB (43). Although some possible PHB inclusion bodies were seen here, the extensive nature of the glycocalyx more likely represents a primary sink for excess carbon metabolism (30). This form of carbon storage differs from mechanisms used by bacteria in older biofilms. In thick biofilms, PHB inclusions can account for up to 50% of the cell volume of the bacteria and appear to be a principal form of carbon storage (31). Biofilm-forming bacteria probably synthesize a glycocalyx for more important functions than as a carbon-storage mechanism. The fact, however, that its synthesis does act as a carbon sink is useful in determining the fate of organic carbon in wastewaters treated by thin biofilms.

In the aqueous environment, the bacterial glycocalyx is both highly hydrated and ordered (20, 44). The glycocalyx, however, is usually radically condensed unless its protein content is high (14) or the structure is stabilized before fixation and dehydration (3, 4). Both the T1 and

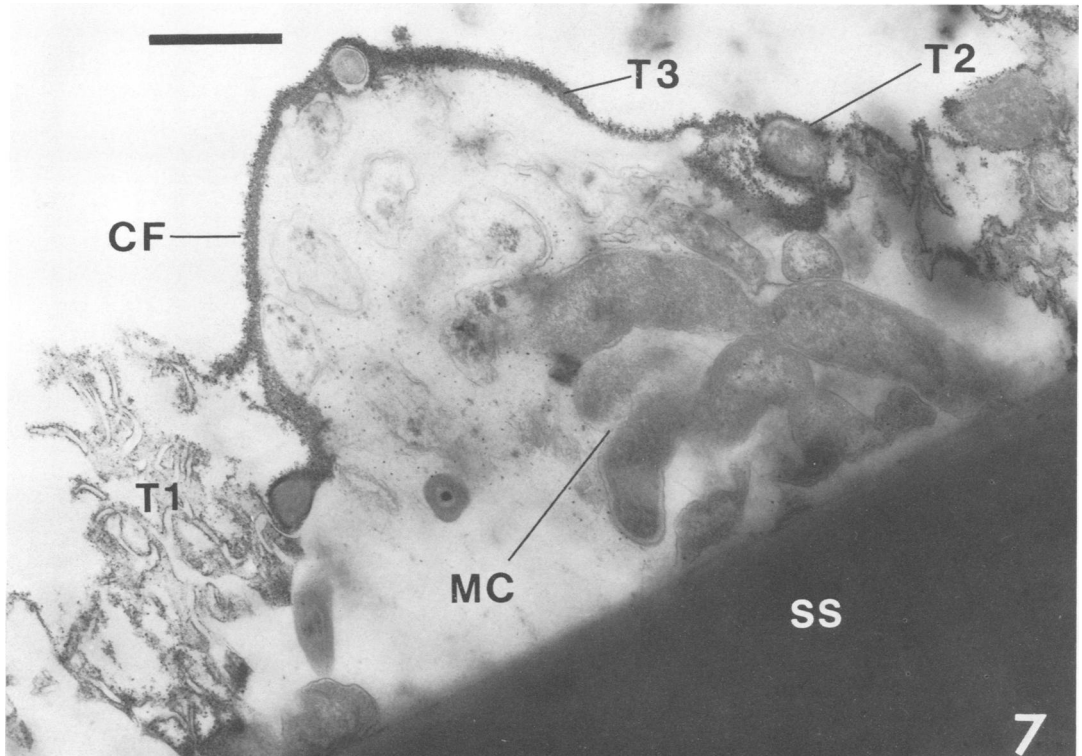


FIG. 7. TEM micrograph of attached biofilm, 144 h old. CF procedure. T1, type 1 glycocalyx; T2, type 2 glycocalyx; T3, type 3 glycocalyx; CF, CF deposition; MC, microcolony composed of gram-negative cells; SS, sampling stub. Bar, 0.5 μm . The glycocalyx appears to mediate attachment. Note the morphologically similar sister cells present within the T3 glycocalyx. Some of the cells appear to be ghost cells. The envelopes of the gram-negative sister cells are convoluted. The T2 glycocalyx appears to be continuous with the T1 and T3 glycocalyxes.

the T3 glycocalyxes may have been composed of sufficient protein to remain dense and resist condensation. Their visualized structure in thin section may have approximated their actual hydrated structure. The T1 glycocalyx was similar in size to a slime layer shown elsewhere (29). The T2 glycocalyx was similar to glycocalyxes found in other types of biofilms (9, 16, 27, 41). The T3 glycocalyx appeared to be similar to common capsules shown in other studies (17, 26, 30, 43). The presence of at least three glycocalyxes in this thin wastewater biofilm is probably the result of the presence of various bacterial species and the different biochemical compositions of the glycocalyxes of the individual species (14, 17). Biofilms from other environments possess different glycocalyx structures within the bacterial assemblage as well (9, 27).

The anionic charge distribution on or within all three types of glycocalyxes was demonstrated with CF. The presence of anionic functional groups within the glycocalyx (48) could account for its apparent polyanionic nature as shown by

its avidity for CF. Rorem (46) found that an extensive glycocalyx was more efficient than a normal glycocalyx in metal ion complexation and removal. Undoubtedly, its dense polyanionic charge distribution is responsible for its adsorptivity (20) and the ability to sequester substrates (30). The extensive nature, however, may constitute a resistance to substrate diffusion to cell transport sites (32).

In conclusion, it would appear that in situ wastewater biofilm formation parallels marine biofilm formation. We have documented two functions of a thin wastewater biofilm glycocalyx. The structure (i) forms a matrix about the bacteria and anchors the biofilm to the substratum and (ii) provides an extensive surface area with polyanionic properties.

ACKNOWLEDGMENTS

We thank Marilyn Ecker of the University of New Hampshire Electron Microscope Facility for the SEM micrographs. The University of New Hampshire Research Office provided funds for photomicrography.

LITERATURE CITED

- Alleman, J. E., J. A. Veil, and J. T. Canaday. 1982. Scanning electron microscope evaluation of rotating biological contactor biofilm. *Water Res.* 16:543-550.
- Balkwill, D. L., and L. E. Casida, Jr. 1979. Attachment to autoclaved soil of bacterial cells from pure cultures of soil isolates. *Appl. Environ. Microbiol.* 37:1031-1037.
- Bayer, M. E., and H. Thurow. 1977. Polysaccharide capsule of *Escherichia coli*: microscope study of its size, structure, and sites of synthesis. *J. Bacteriol.* 130:911-936.
- Birdsell, D. C., R. J. Doyle, and M. Morgenstern. 1975. Organization of teichoic acid in the cell wall of *Bacillus subtilis*. *J. Bacteriol.* 121:726-734.
- Bryers, J. D., and W. G. Characklis. 1982. Processes governing primary biofilm formation. *Biotechnol. Bioeng.* 24:2451-2476.
- Cagle, G. D., R. M. Pfister, and G. R. Vela. 1972. Improved staining of extracellular polymer for electron microscopy: examination of *Azotobacter*, *Zoogloea*, *Leuconostoc*, and *Bacillus*. *Appl. Microbiol.* 24:477-487.
- Characklis, W. G., M. G. Trulear, J. D. Bryers, and N. Zelter. 1982. Dynamics of biofilm processes: methods. *Water Res.* 16:1207-1216.
- Cheng, K.-J., and J. W. Costerton. 1980. The formation of microcolonies by rumen bacteria. *Can. J. Microbiol.* 26:1104-1113.
- Cheng, K.-J., R. T. Irvin, and J. W. Costerton. 1981. Autochthonous and pathogenic colonization of animal tissues by bacteria. *Can. J. Microbiol.* 27:461-490.
- Corpe, W. A. 1980. Microbial surface components involved in adsorption of microorganisms onto surfaces, p. 105-144. *In* G. Bitton and K. C. Marshall (ed.), *Adsorption of microorganisms to surfaces*. John Wiley & Sons, Inc., New York.
- Corpe, W. A. 1974. Periphytic marine bacteria and the formation of microbial films on solid surfaces, p. 397-417. *In* R. R. Colwell and R. Y. Morita (ed.), *Effect of the ocean environment on microbial activities*. University Park Press, Baltimore, Md.
- Costerton, J. W. 1980. Some techniques involved in study of adsorption of microorganisms to surfaces, p. 403-432. *In* G. Bitton and K. C. Marshall (ed.), *Adsorption of microorganisms to surfaces*. John Wiley & Sons, Inc., New York.
- Costerton, J. W., J. M. Ingram, and K.-J. Cheng. 1974. Structure and function of the cell envelope of gram-negative bacteria. *Bacteriol. Rev.* 38:87-110.
- Costerton, J. W., R. T. Irvin, and K.-J. Cheng. 1981. The role of bacterial surface structures in pathogenesis. *Crit. Rev. Microbiol.* 8:303-338.
- Danon, D., L. Goldstein, Y. Marikovskiy, and E. Skutelsky. 1972. Use of cationized ferritin as a label of negative charges on cell surfaces. *J. Ultrastr. Res.* 38:500-510.
- Dazzo, F. B. 1980. Adsorption of microorganisms to roots and other plant surfaces, p. 253-316. *In* G. Bitton and K. C. Marshall (ed.), *Adsorption of microorganisms to surfaces*. John Wiley & Sons, Inc., New York.
- Deinema, M. H., and L. P. T. M. Zevenhuizen. 1971. Formation of cellulose fibrils by gram-negative bacteria and their role in bacterial flocculation. *Arch. Mikrobiol.* 78:42-57.
- Dempsey, M. J. 1981. Marine bacterial fouling: a scanning electron microscope study. *Mar. Biol.* 61:305-315.
- Dias, F. F., and J. V. Bhat. 1964. Microbial ecology of activated sludge. I. Dominant bacteria. *Appl. Microbiol.* 12:412-417.
- Dudman, W. F. 1977. The role of surface polysaccharides in natural environments, p. 357-414. *In* I. W. Sutherland (ed.), *Surface carbohydrates of the prokaryotic cell*. Academic Press, Inc., New York.
- Dunlop, W. F., and A. W. Robards. 1973. Ultrastructural study of poly- β -hydroxybutyrate granules from *Bacillus cereus*. *J. Bacteriol.* 114:1271-1280.
- Ellwood, D. C., C. W. Keevil, P. D. Marsh, C. M. Brown, and J. N. Wardell. 1982. Surface-associated growth. *Philos. Trans. R. Soc. London Ser B* 297:517-532.
- Fletcher, M. 1977. Attachment of marine bacteria to surfaces, p. 407-410. *In* D. Schlessinger (ed.), *Microbiology—1977*. American Society for Microbiology, Washington, D.C.
- Fletcher, M., and G. D. Floodgate. 1973. An electron-microscopic demonstration of an acidic polysaccharide involved in the adhesion of a marine bacterium to solid surfaces. *J. Gen. Microbiol.* 74:325-334.
- Fletcher, M., and G. I. Loeb. 1979. Influence of substratum characteristics on the attachment of a marine pseudomonad to solid surfaces. *Appl. Environ. Microbiol.* 37:67-72.
- Freidman, B. A., P. R. Dugan, R. M. Pfister, and C. C. Remsen. 1968. Fine structure and composition of the zoogloeal matrix surrounding *Zoogloea ramigera*. *J. Bacteriol.* 96:2144-2153.
- Geesey, G. G., W. T. Richardson, H. G. Yeomans, R. T. Irvin, and J. W. Costerton. 1977. Microscopic examination of natural sessile bacterial populations from an alpine stream. *Can. J. Microbiol.* 23:1733-1736.
- Greenawald, J. W., and T. L. Whiteside. 1975. Mesosomes: membranous bacterial organelles. *Bacteriol. Rev.* 39:405-463.
- Jones, H. C., I. L. Roth, and W. M. Sanders. 1976. Electron microscopic study of a slime layer. *J. Bacteriol.* 99:316-325.
- Joyce, G. H., and P. R. Dugan. 1970. The role of flocculating bacteria in BOD removal from wastewater. *Dev. Ind. Microbiol.* 11:377-386.
- Kinner, N. E., D. L. Balkwill, and P. L. Bishop. 1983. Light and electron microscopic studies of microorganisms growing in rotating biological contactor biofilms. *Appl. Environ. Microbiol.* 45:1659-1669.
- Ladd, T. I., J. W. Costerton, and G. G. Geesey. 1979. Determination of the heterotrophic activity of epilithic microbial populations, p. 180-195. *In* J. W. Costerton and R. R. Colwell (ed.), *Native aquatic bacteria: enumeration, activity, and ecology*. American Society for Testing and Materials Press, Philadelphia, Pa.
- La Motta, E. J. 1976. Kinetics of growth and substrate uptake in a biological film system. *Appl. Environ. Microbiol.* 31:286-293.
- Loeb, G. I., and R. A. Neihof. 1975. Marine conditioning films. *Adv. Chem. Ser.* 145:319-335.
- Luft, J. H. 1971. Ruthenium red and violet. I. Chemistry, purification, methods of use for electron microscopy and mechanism of action. *Anat. Rec.* 171:347-368.
- MacAlister, T. J., R. T. Irvin, and J. W. Costerton. 1977. Cell surface-localized alkaline phosphatase of *Escherichia coli* as visualized by reaction product deposition and ferritin-labeled antibodies. *J. Bacteriol.* 130:318-328.
- Marshall, K. C., R. Stout, and R. Mitchell. 1971. Mechanisms of the initial events in the sorption of a marine bacteria to surfaces. *J. Gen. Microbiol.* 68:337-348.
- Marshall, K. C., R. Stout, and R. Mitchell. 1971. Selective sorption of bacteria from seawater. *Can. J. Microbiol.* 17:1413-1416.
- Matson, J. V., and W. G. Characklis. 1976. Diffusion into microbial aggregates. *Water Res.* 10:877-885.
- McCoy, W. F., J. D. Bryers, J. Robbins, and J. W. Costerton. 1981. Observations of fouling biofilm formation. *Can. J. Microbiol.* 27:910-917.
- Newman, H. N. 1980. Retention of bacteria on oral surfaces, p. 207-251. *In* G. Bitton and K. C. Marshall (ed.), *Adsorption of microorganisms to surfaces*. John Wiley & Sons, Inc., New York.
- Ottow, J. C. G. 1975. Ecology, physiology, and genetics of fimbriae and pili. *Annu. Rev. Microbiol.* 29:79-108.
- Parsons, A. B., and P. R. Dugan. 1971. Production of extracellular polysaccharide matrix by *Zoogloea ramigera*. *Appl. Microbiol.* 21:657-661.
- Politis, D. J., and R. N. Goodman. 1980. Fine structure of extracellular polysaccharide of *Erwinia amylovora*. *Appl.*

- Environ. Microbiol. **40**:596–607.
45. **Reynolds, E. S.** 1963. The use of lead citrate at high pH as an electron-opaque stain in electron microscopy. *J. Cell. Biol.* **17**:208–212.
 46. **Rorem, E. S.** 1955. Uptake of rubidium and phosphate ions by polysaccharide-producing bacteria. *J. Bacteriol.* **70**:691–701.
 47. **Spurr, A. R.** 1969. A low-viscosity epoxy resin embedding medium for electron microscopy. *J. Ultrastr. Res.* **26**:31–43.
 48. **Sutherland, I. W.** 1977. Bacterial exopolysaccharides—their nature and production, p. 27–96. *In* I. W. Sutherland (ed.), *Surface carbohydrates of the prokaryotic cell*. Academic Press, Inc., New York.
 49. **Ware, G. C., and J. E. Loveless.** 1958. The construction of biological film in a percolating sewage filter. *J. Appl. Bacteriol.* **21**:308–312.
 50. **Williams, A. G., and J. W. T. Wimpenny.** 1978. Exopolysaccharide production by *Pseudomonas* NCIB 11264 grown in continuous culture. *J. Gen. Microbiol.* **104**:47–57.
 51. **Zevenhuizen, L. P. T. M.** 1981. Cellular glycogen, β -1,2-glucan, poly- β -hydroxybutyric acid and extracellular polysaccharides in fast-growing species of *Rhizobium*. *Antonie van Leeuwenhoek J. Microbiol. Serol.* **47**:481–497.
 52. **Zobell, C. E.** 1943. The effect of solid surfaces upon bacterial activity. *J. Bacteriol.* **46**:39–56.